Velocity-Matched Distributed Photodetectors and Balanced Photodetectors with p-i-n Photodiodes

M. Saif Islam, *Student Member, IEEE*, Sanjeev Murthy, *Student Member, IEEE*, Tatsuo Itoh, *Fellow, IEEE*, Ming C. Wu, *Senior Member, IEEE*, Dalma Novak, *Member, IEEE*, Rodney B. Waterhouse, *Member, IEEE*, Deborah L. Sivco, and Alfred Y. Cho, *Fellow, IEEE*

***Abstract*—We report on the first demonstration of velocity-matched distributed photodetectors and balanced photodetectors with p-i-n photodetectors. Record-high linear dc photocurrent of 45 mA has been achieved without suffering from thermal damage, thanks to the superior power handling capability of p-i-n photodiodes. A novel fiber alignment technique has been developed to achieve high linear photocurrent. More than 37 dB of common-mode-rejection ratio and 45-dB suppression of laser relative intensity noise over a broad frequency range have been achieved using the distributed balanced photodetectors in an RF fiber-optic link. The frequency response is flat from 1 to 35 GHz.**

***Index Terms*—Analog fiber-optic links, balanced photodetectors, high power photodetector, microwave photonics, noise suppression, optical receivers, p-i-n photodetectors, RF photonics.**

I. Introduction

IN AN externally modulated fiber-optic link, high-speed photodetectors (PDs) with high saturation photocurrent can improve the overall link performance, including the link gain, noise figure, and spurious free dynamic range (SFDR) [1]. When PDs have sufficiently high saturation power, this improvement is limited by the relative intensity noise (RIN) of the laser source and the amplified spontaneous emission noise (ASE) from erbium-doped fiber amplifiers (EDFA). It is known that the laser RIN and EDFA-added noise can be suppressed by balanced receivers [1], [2]. High power balanced receivers are also important for optical heterodyned receivers and optoelectronic generation of high power microwaves and millimeter-waves. Therefore, PDs and, in particular balanced PDs with high linear photocurrent are critical components of high-performance RF photonic links [1]–[3].

Several approaches have been proposed to increase the maximum linear photocurrent of high-speed PDs, including waveguide PDs with low confinement factors [4]–[6], traveling-wave photodetectors [7], [8] phototransistors [9], uni-traveling-carrier photodiode [10], and velocity-matched distributed photodetectors (VMDP) [11]–[13], and parallel fed VMDP [14]. Using the VMDP with metal–semiconductor–metal (MSM) PDs, we have previously achieved a saturation photocurrent of 33 mA at 1.55-μm wavelength [15]. Bimberg *et al.* also reported on an MSM-based VMDP with a bandwidth above 78 GHz [13]. We have also demonstrated a novel monolithic distributed balanced photodetector with MSM PDs [16] that successfully suppressed broad band (1–12 GHz) laser RIN [17]. Maximum noise suppression of 36 dB was observed at the relaxation oscillation frequency of the DFB laser.

The maximum linear photocurrent in our MSM-VMDP was limited by the catastrophic damage caused by thermal runaway. p-i-n PDs have higher threshold for thermal runaway than MSM PDs. It was previously shown that MSM PDs fail at junction temperatures of $\sim$700 K [18], whereas p-i-n can stand junction temperatures above 900 K [19]. We developed a theoretical model to carry out detailed analysis of the thermal runaway issues and found that the dark current ($I_{\rm dark}$) and the effective barrier height ($q\phi_b$) are the fundamental parameters in the failure mechanism of high power PDs. Our investigation also showed that junction PDs (such as p-i-n) with high $q\phi_b$ were expected to perform better than metal–semiconductor contact PDs (such as MSM or Schottky) for high power operation. Further details of our analysis are reported elsewhere [20]. The uniform electric field distribution in p-i-n is also advantageous for linear operation under high power illumination. Moreover, the fabrication of high bandwidth MSM PDs demands sophisticated submicron *e*-beam writing and thin MSM fingers are vulnerable to failure caused by high photocurrents. Therefore, VMDP with p-i-n PDs are of great interest for high power photodetection.

In this paper, we report on the first demonstration of the VMDP with p-i-n PDs. Record-high linear photocurrent of 45 mA has been achieved. No thermal runaway was observed for photocurrent above 55 mA. We have also found that the fiber position for maximum responsivity is different from that for maximum linear photocurrent. A novel technique of offset launching of the input power helped attain more uniform distribution of photocurrents. Our VMDP has a flat frequency response up to 35 GHz, though there is an initial drop at low frequency due to slow carrier diffusion. We also fabricated a distributed balanced photodetectors with p-i-n PDs and successfully suppressed broad-band RIN and EDFA added noises by more than 43 dB.

Manuscript received January 22, 2001; revised May 28, 2001. This work was supported in part by Office of Naval Research under a Multiuniversity Research Initiative on RF photonics, and the University of California Microelectronics Innovation and Computer Research Opportunities.

M. S. Islam was with the Electrical Engineering Department, University of California at Los Angeles, Los Angeles CA 90095 USA. He is now with Optical Network Research, JDS Uniphase Corporation, Santa Clara, CA 95054 USA (e-mail: saif.islam@jdsuniphase.com).

S. Murthy, T. Itoh, and M. C. Wu are with the Electrical Engineering Department, University of California at Los Angeles, Los Angeles, CA 90095 USA.

D. Novak and R. B. Waterhouse are with the Australian Photonics Cooperative Research Center, Department of Electrical and Electronic Engineering, The University of Melbourne, Melbourne, Vic. 3010, Australia.

D. L. Sivco and A. Y. Cho are with Lucent Technologies, Bell Laboratories, Murray Hill, NJ 07974 USA.

Publisher Item Identifier S 0018-9480(01)08713-0.

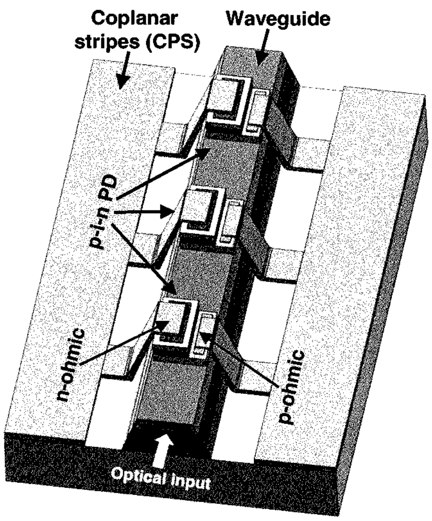

Fig. 1. Schematic of the VMDP showing the passive optical waveguide, active p-i-n PDs and microwave transmission line.

II. Design and Fabrication

The schematic structure of the VMDP is illustrated in Fig. 1. A linear array of p-i-n PDs is periodically distributed on top of a passive optical waveguide. Optical signal is evanescently coupled from the passive waveguide to the active p-i-n PDs. Photocurrent generated from the individual PDs are added in phase through a coplanar strips (CPS) microwave transmission line that is velocity-matched to the optical velocity in the waveguide. The characteristic impedance of the perodically loaded transmission line is designed to have a value of 50 Ω. The PDs are kept below saturation by coupling only a small fraction of optical power to each PDs.

The optical waveguide was grown with following layers: a 400-nm-thick $In_{0.52}Al_{0.36}Ga_{0.12}As$ lower cladding layer, a 600-nm-thick $In_{0.52}Al_{0.269}Ga_{0.211}As$ core region, a 200-nm-thick $In_{0.52}Al_{0.36}Ga_{0.12}As$ first upper cladding layer that has a Be doping concentration of 5×10^{17} cm^{-3} in the upper half; a 150-nm-thick $In_{0.52}Al_{0.48}As$ second upper cladding layer with a doping concentration of 5×10^{18} cm^{-3} and a 150-nm-thick $In_{0.52}Al_{0.382}Ga_{0.98}As$ as third upper cladding layer that was gradually increased in doping to a concentration of 1×10^{19} cm^{-3} at the top of the layer. A 10-nm-thick $In_{0.52}Ga_{0.47}As$ layer with a Be doping concentration $>1 \times 10^{19}$ cm^{-3} was used on this layer for p-ohmic contacts. The 250-nm-thick absorption region is located on top of the passive waveguide for evanescent coupling. Finally, a 200-nm-thick $In_{0.52}Al_{0.382}Ga_{0.98}As$ with a Si doping concentration $>1 \times 10^{19}$ cm^{-3} was employed for n-ohmic contacts. Graded layers are incorporated in the structure to reduce the minority carrier trapping at heterointerfaces.

The fabrication process is described in the following: First, the PD mesas were isolated by etching away the active layers from the wafer except from the places where PDs are located. Top n-ohmic and bottom p-ohmic contact metals were then deposited and lifted-off. A rapid thermal annealing (RTA) process at 410 °C for 10 s is performed to reduce the contact resistance of the device. A Si_3N_4 etch mask was deposited by plasma-enhanced chemical vapor deposition (PECVD). Optical ridge waveguide with a 1.5-μm depth was formed by wet chemical etching. Special care has been taken to ensure the smooth, continuous transition between the passive waveguides and the active PD sections. After defining the waveguides, Si_3N_4 was removed using buffered HF (BOE). A thin PECVD Si_3N_4 film of 1500-Å thickness was then deposited all over the sample to achieve three purposes. First, it covers the mesa walls and thus prevents the interconnect metals from touching the InGaAs layer—a potential contributor of high dark current in a PD. Second, it passivates the surface of the wafer, and finally it serves as the dielectric layer between the CPS transmission lines and the substrate, which eliminates the leakage current between the CPS. The CPS transmission lines were formed by standard lift-off process to connect the distributed PDs.

To increase the fiber coupling efficiency [21], the optical waveguide is designed to have a large optical core in the vertical direction. Multimode waveguide in the lateral direction is employed so that the PD and its contacts can be placed on top of the waveguide. As will be shown later, this design can minimize the optical loss at waveguide/PD transition. However, in a multimode waveguide, different mode propagates at different velocities. Thus, the microwave velocity can only be matched to the group velocity of only one optical mode. Thus there is some inherent velocity mismatch in multimode devices. However, the mismatch is small (<10%) and the bandwidth limit due to velocity mismatch is greater than 150 GHz, which is much higher than the transit time-limited bandwidth of our current device. Moreover, our beam propagation method (BPM) simulation shows that more than 90% of the input power is coupled to the fundamental mode. When the design target goes above 100 GHz, the single-mode waveguide will ensure better performance.

III. Device Characteristics

The dc responsivity is 0.42 A/W at 1-V bias without antireflection (AR) coating. This responsivity can be further improved by employing air-bridges to connect PDs with the microwave transmission line, which prevent direct metal deposition on the sidewalls of the waveguide. The reverse bias breakdown is ~1.5 V. The low breakdown is caused by the diffusion of p-type dopants from the lower contact layers into the InGaAs absorbing layer during the epitaxial growth. The fiber coupling efficiency can be improved by integrating a spot-size converter for better mode-matching with fiber. Coupling efficiency as high as 90% has been reported [22]. With both AR coating and spot size converter, the responsivity can potentially be increased to 0.9 A/W. The spot-size converters also reduce the optical power density at facets and therefore increase the optical damage power level. The microwave characteristics of the loaded CPS is measured by a HP 8510C network analyzer. The measured characteristic impedance matches very well to 50 Ω (within 3%) for a broad frequency range.

One of the main tradeoffs in the design of p-i-n VMDP is the placement of Ohmic contacts. Fig. 2 shows three different contact schemes: (a) parallel contacts on a continuous waveguide; (b) tandem contacts on a continuous waveguide; and (c) parallel contacts with lower contact outside the waveguide. The contact

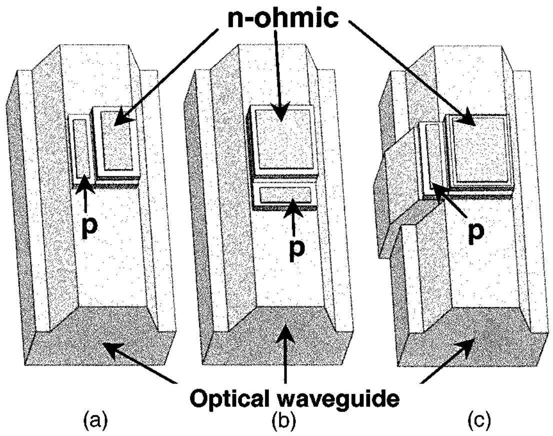

Fig. 2. Schematic of three different contact schemes. (a) Parallel on continuous waveguide. (b)Tandem on continuous waveguide. (c) Parallel contacts with lower contact outside the waveguide.

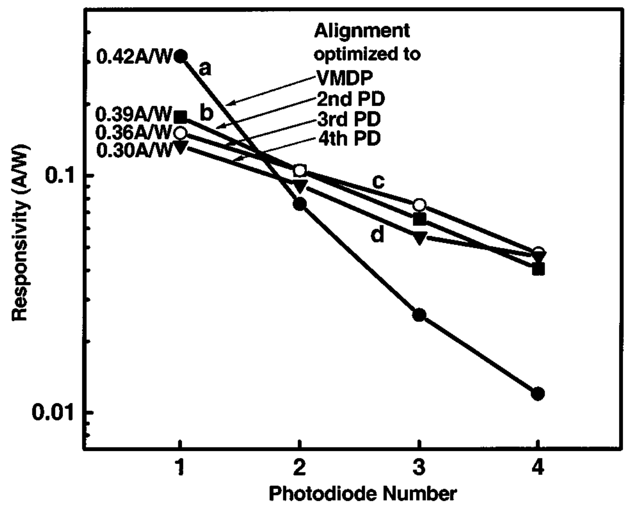

Fig. 3. Measured responsivity of each PDs in the split contact VMDP. Trace a shows the data for optimized alignment to the VMDP for highest responsivity. Trace b, c, and d show data for optimizing the fiber alignment to the second, third, and fourth PD in the array.

area for each PD is $20 \times 2.5\ \mu\text{m}^2$. The spacing between the n and p contacts is 2 μm. In our device, the p-ohmic contact is the lower contact, which is close to the core of the passive waveguide. We experimentally investigated the performances of the VMDPs with different contact schemes. Our results show that contact scheme (a) exhibits the best performance with the lowest loss and more uniform photocurrent distribution along the PD array. This geometry ensures the highest responsivity (0.42 A/W) and linearity (more than 45 mA).

The tandem contacts on continuous waveguide are not efficient for guiding light to distant PDs. The presence of p-metal on top of waveguide causes high optical loss. Moreover, during the thermal annealing process, part of the p-metal is diffused into the upper cladding of the waveguides. This causes additional free carrier absorption. We measured the lowest responsivity of ~0.22 A/W and linear photocurrent of ~5 mA in the devices with this type of contacts.

In scheme (c) that has parallel contacts with the lower contact outside the waveguide, lateral discontinuity in the waveguide introduces excessive optical loss. As a result, most of the propagating power is lost at the PD-waveguide interface. Although the responsivity is only slightly lower (0.36 A/W) than that of scheme (a), the linear photocurrent is much lower (~10 mA) in this configuration. The PDs beyond the first one in the VMDP receives negligible power, and thus the maximum linear photocurrent of the VMDP remains limited by the first PD.

To characterize the distribution of photocurrents within the VMDP, we fabricated test VMDPs with separate electrical contacts for each PDs. The measurement results are shown in Fig. 3. When the fiber is positioned to optimize the overall responsivity of the VMDP (0.42 A/W), the responsivity distribution has a very steep decay [Fig. 3, line a]. The *first* PD contributed 73.8% of the total photocurrent. The maximum linear photocurrent is 22 mA. If the fiber is moved in the vertical direction to optimize the response of the *second* PD instead of the entire VMDP, more uniform distribution of photocurrent is obtained. The responsivity of the overall VMDP decreased slightly to 0.39 A/W, [Fig. 3, line b] however, the maximum linear photocurrent increased to 35 mA. This is because more PDs are contributing to the total photocurrent when the first PD reaches saturation. If we move the fiber again to optimize response of the third PD, the maximum linear photocurrent of the VMDP is increased further to 45.5 mA. The overall responsivity became 0.36 A/W. The distribution of responsivity under this coupling condition is shown in Fig. 3, line c. The offsets of the fiber position for lines b and c are ~0.09 and ~0.21 μm, respectively, in the vertical direction, with reference to the fiber position for (a). Aligning the input power to optimize the photocurrent of a further distant PD (such as the fifth or sixth one) makes the power distribution more uniform. Moving the fiber in the later direction has little effect on the distribution of photocurrents.

Careful observation of Fig. 3 reveals two different slopes for the photocurrent distribution. When the input power is aligned for optimum responsivity of the VMDP, the slope of the curve is very high indicating a fast decay of the input power. As we move the fiber to optimize the alignment to second PD in the array, the slope abruptly reduces to a lower value. When the fiber is aligned to optimize the responsivities of the third or fourth PD, the slope of the curves in Fig. 3 keeps decreasing slowly, resulting in a more uniform distribution of the optical power.

The explanation for the above observation is as follows. Because the first photodiodes is located very close to the facet (100 μm away), the optical field coupled into VMDP has not reached the steady state distribution yet. The transient field can be directly coupled into the photodiodes, resulting in higher photocurrents in the first photodiode. Therefore, when we align the fiber by maximizing the overall response of the VMDP, the fiber-to-waveguide coupling is actually not optimized. Though the absorption of the transient field helps increase the overall quantum efficiency, the extra photocurrent concentrates in the first photodiode and causes it to saturate at lower overall photocurrent. The photocurrents of the photodiodes farther away from the input facet are less influenced by the transient field and, therefore, are better monitors for the fiber alignment.

An alternative explanation of the alignment sensitive intensity distribution over different photodiodes is coupling to different waveguide modes. Though our waveguide was designed to be

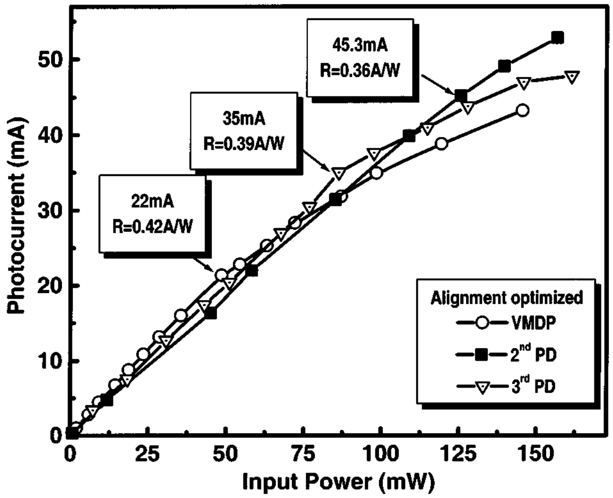

Fig. 4. Measured dc linear photocurrents for three different input fiber positions. The linear current improves greatly when the input power is optimized to a distant photodiode.

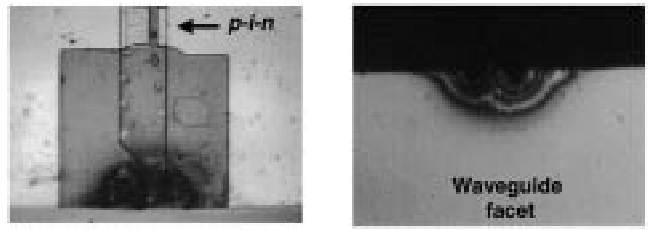

Fig. 5. Burnt facet of a VMDP after more than 200 mW of power is coupled to the passive waveguide. Top view is on the left and edge view is on the right. The device electrical characteristics remain unchanged even after the facet burn.

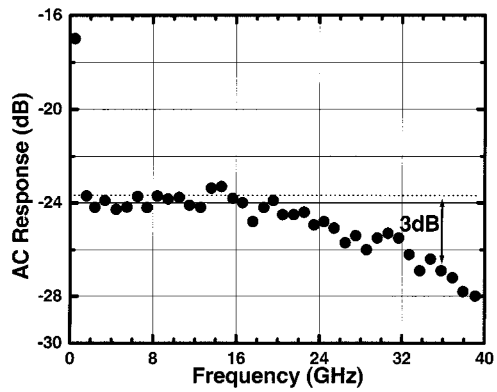

Fig. 6. Measured frequency response of the p-i-n VMDP with optical heterodyning. Neglecting the sharp rolloff below 1 GHz, the device has a 3-dB bandwidth >35 GHz.

single mode, it was very close to the cutoff of the second mode. Due to variation of epitaxial growth, it is possible our waveguide could support two modes. Coupling to different modes could also result in different photocurrent distribution over different photodiodes. More detailed analysis is needed to identify the exact mechanism.

Fig. 4 shows the photocurrent versus optical power for the three alignment schemes: a) maximum overall responsivity; b) maximum photocurrent for the second PD; and c) maximum photocurrent for the third PD. The maximum linear photocurrent of 45 mA was obtained for scheme c). To our knowledge, this is the highest linear dc photocurrent reported in high-frequency photodetectors.

Our finding also suggests new VMDP structures with built-in monitor PDs for optimum fiber alignment. The photocurrent of a PD farther away from the input facet can be used as a better monitor for the fiber alignment. In addition to the regular array of PDs of the VMDP, we can add an additional monitoring PD in the middle of the waveguide (e.g., between the fourth and the fifth PDs). By optimizing the photocurrent of the monitoring PD, we can ensure high linear photocurrent in the device. The photocurrent distribution can be made even more uniform by tapering the optical coupling between the waveguide and the photodiodes [5], or by splitting power equally to a parallel array of photodiodes as in the parallel-fed VMDP [14].

In contrast to the MSM VMDP we reported previously [14], the p-i-n VMDP does not fail at the maximum linear photocurrent. In fact, our device survives at photocurrent as high as 55 mA. If we continue to increase the photocurrent, eventually the facet of the optical waveguide is damaged at 200 mW. Even under this circumstance, the active PDs of the p-i-n VMDP remains undamaged. In fact, we can couple light in from the undamaged facet at the other end, and obtain the same level of maximum linear photocurrent as before. Fig. 5 shows the top-view and side-view photograph of a burnt facet when more than 200 mW of input power is launched into the waveguide. It can be seen that the damage is localized at the facet. A spot-size converter can reduce the input power density and increase the threshold power for facet burn.

We used both frequency and time domain measurements to characterize the ac response of the VMDP. The frequency domain measurement was performed by optical heterodyning method using two external cavity tunable lasers at 1550 nm. The optical signals are combined by a 3-dB coupler, and coupled to the VMDP through a fiber pickup head. The output is collected by a 50-GHz probe and monitored by an RF power meter. The calibrated frequency response of the VMDP is shown in Fig. 6. The ac response has a quick rolloff at low frequencies (below 1 GHz) and then remains almost flat. The initial rolloff (~7 dB) at low frequency is due to the slow carrier diffusion in the active region, which is caused by unintentional migration of p-dopants (Be) during epitaxial growth. Excluding the low frequency rolloff, the 3-dB frequency is 35 GHz. The ac quantum efficiency is 3.5 dB lower than the dc quantum efficiency. The maximum linear ac photocurrent will be reduced to ~20 mA. Therefore, it is important to eliminate the low frequency rolloff.

The low frequency rolloff can be eliminated by inserting an undoped setback layer in the p-cladding layer. The breakdown voltage of the PD can also be increased. Devices using the new epitaxial structures are now being fabricated. Another issue of our current devices is the high contact resistance of the lower Ohmic contact, which results in low *RC*-limited bandwidth. Our current epitaxial layer structure does not have an effective stop etch layer before the lower Ohmic contact layer. As a result, the contact is actually formed on the InGaAlAs layer with low

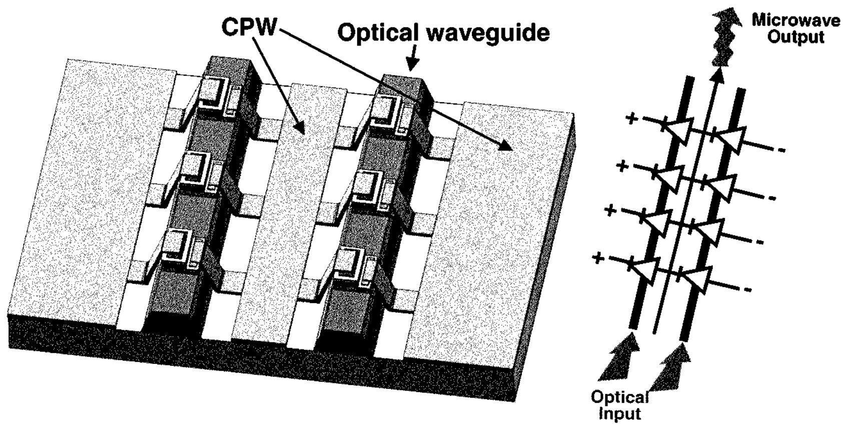

Fig. 7. Schematic structure and principle of the distributed balanced photodetector. Multiple balanced photodetector pairs are cascaded in series along a CPW to increase saturation photocurrent. The p-i-n PDs provide the capacitance and resistance to the CPW and help to slow down the microwave velocity of the receiver matching it to that of optical velocity.

p-doping concentration. In the new epitaxial layer design, we have inserted a stop etch layer to improve the contact resistance. The new device should exhibit higher frequency response.

IV. Distributed Balanced PDs

We designed a distributed balanced photodetector structure using p-i-n PDs. Fig. 7 shows the schematic and the basic principle of the device. It consists of two input optical waveguides, two arrays of high-speed p-i-n PDs distributed along two passive optical waveguides, and a coplanar waveguide (CPW) microwave transmission line with a characteristic impedance of 50 Ω when loaded. The detector operates in balanced mode when a voltage bias is applied between the two ground electrodes of the CPW. The PD arrays provide periodic capacitance loading to slow down the microwave velocity. By adjusting the length and separation of the PDs, velocity matching between the CPW and the optical waveguides is achieved. Detailed description of a similar device with MSM PDs, experimental setup, biasing scheme, several references on balanced detectors and typical fiber-optic links with balanced detectors were reported in [16]. A more recent work on waveguide fed monolithically integrated balanced detectors have been reported by Unterboersch *et al.* [23].

The common-mode-rejection-ratio (CMRR) is an important parameter of a balanced receiver when high RIN suppression is considered. CMRR, defined as $\mathrm{CMRR} = 20 \cdot \log(i_{\mathrm{COM}}/i_{\mathrm{DIFF}})$ (where, i_{COM} is the total current and i_{DIFF} is the difference in the magnitude of the photocurrent of the individual PDs), indicates how well matched the PDs are in the receiver. Fig. 8 depicts the measured CMRR versus photocurrent. Very high CMRR (>37 dB) was obtained for a wide range of photocurrents (from a few nA to 31 mA). This is attributed to the well-matched characteristics of the PDs in our monolithic balanced detectors.

Fig. 9 shows the RF spectra of the output from a distributed balanced receiver in the unbalanced (only one waveguide is illuminated) and the balanced mode using the test setup described in [17]. Suppression of the noise floor by 43 dB has been observed in the balanced mode over a wide frequency range from a few megahertz to 8 GHz with a total photocurrent of 31 mA on each array of the receiver. The RIN suppression is slightly higher than the CMRR shown in Fig. 8 because we fined-tuned the optical input to each waveguide to maximize the RIN suppression. To our knowledge, this is the highest suppression of RIN noise by balanced photodetectors at high frequencies. Shot-noise-limited

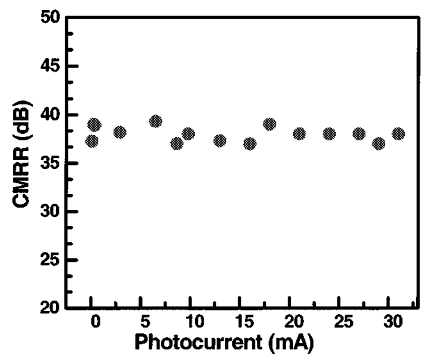

Fig. 8. CMRR versus photocurrent for the distributed balanced receiver. The high CMRR results from the closely matched photodiode characteristics of the individual p-i-n diodes.

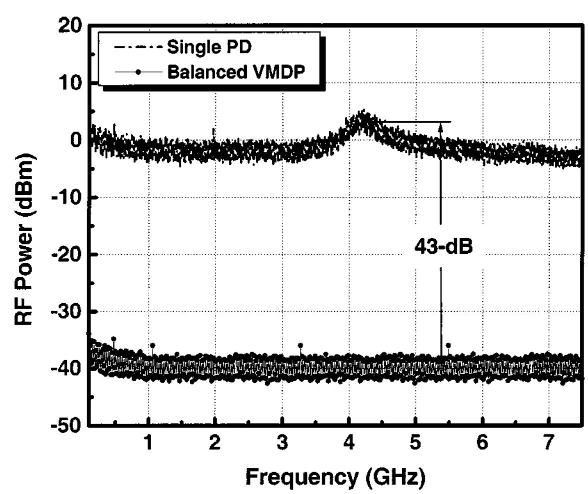

Fig. 9. The noise spectra of a DFB laser measured by the distributed balanced photodetector in unbalanced mode (upper trace) and balanced mode (lower trace). The receiver suppresses RIN noise by more than 43 dB and reaches the shot noise floor.

performance has been achieved at high photocurrent by canceling out the laser RIN.

V. Conclusion

We have successfully demonstrated a velocity-matched distributed photodetector with p-i-n PDs. A high linear dc photocurrent of 45 mA has been achieved. In order to increase the dc linear photocurrents, a novel alignment technique is proposed and demonstrated. The VMDP has a flat frequency response from 1 to 35 GHz. A low frequency rolloff due to slow carrier diffusion is also observed. Distributed balanced photodetectors have also been fabricated and a record high suppression (43 dB) of laser RIN over a broad frequency range has been achieved. We are now in the process of fabricating a new epitaxial structure to eliminate the long diffusion tail and improve the contact resistance.

Acknowledgment

The authors would like to acknowledge T. Jung, University of California at Los Angeles (UCLA), and S. Mathai, UCLA, for their help.

References

[1] C. H. Cox, III, G. E. Betts, and L. M. Johnson, "An analytic and experimental comparison of direct and external modulation in analog fiber-optic links," *IEEE Trans. Microwave Theory Tech.*, vol. 38, pp. 501–509, May 1991.

[2] L. T. Nichols, K. J. Williams, and R. D. Esman, "Optimizing the ultra-wide-band photonic link," *IEEE Trans. Microwave Theory Tech.*, vol. 45, pp. 1384–1389, Aug. 1997.

[3] R. F. Kalman, J. C. Fan, and L. G. Kazovsky, "Dynamic range of coherent analog fiber-optic links," *J. Lightwave Technol.*, vol. 12, pp. 1263–1277, July 1994.

[4] D. C. Scott, T. A. Vang, J. Elliott, D. Forbes, J. Lacey, K. Everett, F. Alvarez, R. Johnson, A. Krispin, J. Brock, L. Lembo, H. Jiang, D. S. Shin, J. T. Zhu, and P. K. L. Yu, "Measurement of IP3 in p-i-n photodetectors and proposed performance requirements for RF fiber-optic links," *IEEE Photon. Technol. Lett.*, vol. 12, p. 422, Apr. 2000.

[5] S. Jasmin, N. Vodjdani, J.-C. Renaud, and A. Enard, "Diluted and distributed-absorption microwave waveguide photodiodes for high efficiency and high power," *IEEE Trans. Microwave Theory Tech.*, vol. 45, pp. 1337–1341, Aug. 1997.

[6] A. R. Williams, A. L. Kellner, X. S. Jiang, and P. K. L. Yu, "InGaAs/InP waveguide photodetector with high saturation intensity," *Electron. Lett.*, vol. 28, no. 24, pp. 2258–919, 1992.

[7] K. S. Giboney, M. J. W. Rodwell, and J. E. Bowers, "Traveling-wave photodetector theory," *IEEE Trans. Microwave Theory Tech.*, vol. 45, pp. 1310–1319, Aug. 1997.

[8] M. Alles, U. Auer, F.-J. Tegude, and D. Jager, "Distributed velocity-matched 1.55 μm InP traveling-wave photodetectors for generation of high millimeterwave signal power," in *IEEE MTT-S Dig.*, 1998, p. 1233.

[9] D. C. Scott, D. P. Prakash, H. Erlig, D. Bhattacharya, M. E. Ali, H. R. Fetterman, and M. Matloubian, "High-power high-frequency traveling-wave heterojunction phototransistors with integrated polyimide waveguide," *IEEE Microwave Guided Wave Lett.*, vol. 8, pp. 284–6, Aug. 1998.

[10] N. Shimizu, Y. Miyamoto, A. Hirano, K. Sato, and T. Ishibashi, "RF saturation mechanism of InP/InGaAs unitravelling-carrier photodiode," *Electron. Lett.*, vol. 36, pp. 750–751, Apr. 2000.

[11] L. Y. Lin, M. C. Wu, T. Itoh, T. A. Vang, R. E. Muller, D. L. Sivco, and A. Y. Cho, "High-power high-speed photodetectors-design, analysis and experimental demonstration," *IEEE Trans. Microwave Theory Tech.*, vol. 45, pp. 1320–1331, Aug. 1997.

[12] T. Chau, L. Fan, D. T. K. Tong, S. Mathai, M. C. Wu, D. L. Sivco, and A. Y. Cho, "Long wavelength velocity-matched distributed photodetectors for RF fiber optic links," *Electron. Lett.*, vol. 34, no. 14, pp. 1422–4, July 1998.

[13] E. Droge, E. H. Bottcher, S. Kollakowski, A. Strittmatter, D. Bimberg, O. Reimann, and R. Steingruber, "78 GHz distributed InGaAs MSM," *Electron. Lett.*, vol. 34, no. 23,, pp. 2241–3, 1998.

[14] S. Murthy, T. Jung, T. Chau, M. C. Wu, D. L. Sivco, and A. Y. Cho, "A novel monolithic distributed traveling wave photodetector parallel optical feed," *IEEE Photon. Technol. Lett.*, vol. 12, pp. 681–683, June 2000.

[15] M. S. Islam, T. Jung, S. Mathai, T. Chau, A. Rollinger, T. Itoh, M. C. Wu, D. L. Sivco, and A. Y. Cho, "High power distributed balanced photo-detectors with high linearity," in *Int. Microwave Photon. Conf.*, Melbourne, Australia, Nov. 16–19, 1999.

[16] M. S. Islam, T. Chau, A. Nespola, S. Mathai, A. R. Rollinger, W. R. Deal, T. Itoh, M. C. Wu, D. L. Sivco, and A. Y. Cho, "Distributed balanced photodetectors for high performance RF photonic links," *IEEE Photon. Technol. Lett.*, vol. 11, pp. 457–560, Apr. 1999.

[17] M. S. Islam, T. Chau, S. Mathai, T. Itoh, M. C. Wu, D. L. Sivco, and A. Y. Cho, "Distributed balanced photodetectors for broad-band noise suppression," *IEEE Trans. Microwave Theory Tech.*, vol. 47, pp. 1282–1288, July 1999.

[18] A. Nespola, T. Chau, M. Pirola, M. C. Wu, G. Ghione, and C. U. Naldi, "Failure analysis of travelling wave MSM distributed photodetectors," in *Int. Electron Dev. Mtg.*, San Francisco, CA, Dec. 6–9, 1998.

[19] K. J. Williams and R. D. Esman, "Design considerations of high-current photodetectors," *J. Lightwave Technol.*, vol. 17, pp. 1443–1454, Aug. 1999.

[20] M. S. Islam, T. Jung, A. Nespola, T. Itoh, M. C. Wu, D. L. Sivco, and A. Y. Cho, "High power and highly linear monolithically integrated distributed balanced photodetectors," *J. Lightwave Technol.*, 2001, submitted for publication.

[21] K. Kato, S. Hata, K. Kawano, J. Yoshida, and A. Kozen, "A high efficiency 50 GHz InGaAs multimode waveguide photodetector," *IEEE J. Quantum Electron.*, vol. 28, pp. 2728–2735, Dec. 1992.

[22] A. Umbach, D. Trommer, R. Steingruber, A. Seeger, W. Ebert, and G. Unterborsch, "Ultrafast, high-power 1.55 μm side-illuminated photodetector with integrated spot size converter," in *OFC 2000*, Baltimore, MD.

[23] G. Unterborsch, C. Schramm, R. Hubsch, G. G. Mekonnen, A. Seeger, D. Trommer, and A. Umbach, "1.55 μm balanced mixer receiver OEIC with 15 GHz bandwidth," in *25th European Opt. Commun. Conf.*, Nice, France, Sept. 26–30, 1999.

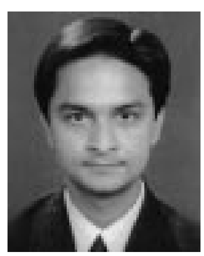

M. Saif Islam (S'98) received the B.Sc. degree in physics from Middle East Technical University (METU), Ankara, Turkey, in 1994, the M.Sc. degree in physics from Bilkent University, Ankara, Turkey, in 1996, and the M.S. and Ph.D. degrees in electrical engineering from the University of California at Los Angeles (UCLA) in 1999 and 2001, respectively.

He joined the Integrated Photonics Laboratory, UCLA in 1997. In January 2001, he joined SDL Inc., Santa Clara, CA, as a Research Scientist with the Technology Development Group. Following the merger of SDL Inc. with the JDS Uniphase Corporation, he is currently with the Optical Network Research Group, Santa Clara, CA, where he conducts research on RZ transmission systems and issues related to Raman pump modules. He has authored or co-authored more than 30 papers in technical journals and refereed conferences and contributed one book chapter. His other research interests include design, fabrication, and characterization of ultrafast resonant-cavity enhanced photodetectors, high-power and high-bandwidth photodetectors, integrated optoelectronic devices, integrated microwave photonic devices including velocity-matched distributed photodetectors (VMDP), and distributed balanced photodetectors and their applications in high-performance RF photonic systems.

Dr. Islam is a member of American Physical Society and Optical Society of America. He received the Student of the Year Award in 1988 from Bangladesh National Student Foundation at UK and the Chancellor's Award in 1989 for securing the first position in the HSC examination among all education boards in Bangladesh. He held the Chancellor's Dissertation Year Fellowship in 2000. He is a recipient of the IEEE Laser and Electro-Optic Society (LEOS) Graduate Student Fellowship Award 2000.

Sanjeev Murthy (S'98) received the B.Tech. degree in electronics and communication engineering from the Indian Institute of Technology, Madras, India, in 1994, the M.S. degree in electrical engineering from the University of California at Los Angeles (UCLA) in 1999, and is currently working toward the Ph.D. degree in electrical engineering at UCLA.

His current research is on velocity matched distributed photodetectors with monolithically integrated multimode interference couplers to achieve high power and high bandwidth. He is also working on high-power terahertz generation through optical heterodyne methods. His other research interests include waveguide devices, integrated optoelectronic devices, integrated microwave photonic devices, and mode-locked lasers.

Tatsuo Itoh (M'69–SM'74–F'82) received the Ph.D. degree in electrical engineering from the University of Illinois at Urbana-Champaign, in 1969.

From September 1966 to April 1976, he was with the Electrical Engineering Department, University of Illinois at Urbana-Champaign. From April 1976 to August 1977, he was a Senior Research Engineer in the Radio Physics Laboratory, SRI International, Menlo Park, CA. From August 1977 to June 1978, he was an Associate Professor with the University of Kentucky, Lexington. In July 1978, he joined the faculty of The University of Texas at Austin, where he became a Professor of electrical engineering in 1981 and Director of the Electrical Engineering Research Laboratory in 1984. During the summer of 1979, he was a Guest Researcher at AEG-Telefunken, Ulm, Germany. In September 1983, he was selected to hold the Hayden Head Centennial Professorship of Engineering at The University of Texas. In September 1984, he was appointed Associate Chairman for Research and Planning of the Electrical and Computer Engineering Department at The University of Texas. In January 1991, he joined the University of California at Los Angeles (UCLA) as Professor of electrical engineering and Holder of the TRW Endowed Chair in Microwave and Millimeter Wave Electronics. He was an Honorary Visiting Professor at Nanjing Institute of Technology, Nanjing, China and at the Japan Defense Academy. In April 1994, he was appointed as Adjunct Research Officer for the Communications Research Laboratory, Ministry of Post and Telecommunication, Japan. He currently holds a Visiting Professorship at the University of Leeds, Leeds, U.K. and is an External Examiner of Graduate Program of the City University of Hong Kong. He has authored or co–authored 274 journal publications, 540 refereed conference presentations, and 30 books/book chapters in the area of microwaves, millimeter-waves, antennas and numerical electromagnetics. He generated 49 Ph.D. students.

Dr. Itoh is a member of the Institute of Electronics and Communication Engineers (IEICE), Japan, and Commissions B and D of USNC/URSI. He served as the editor-in-chief of the IEEE TRANSACTIONS ON MICROWAVE THEORY AND TECHNIQUES from 1983 to 1985. He serves on the Administrative Committee ofthe IEEE Microwave Theory and Techniques Society (IEEE MTT-S). He was vice president of the IEEE MTT-S in 1989 and president in 1990. He was the editor-in-chief of the IEEE MICROWAVE AND GUIDED WAVE LETTERS from 1991 to 1994. He was elected an Honorary Life Member of the IEEE MTT-S in 1994. He was the chairman of USNC/URSI Commission D from 1988 to 1990, and chairman of Commission D of the International URSI from 1993 to 1996. He is chair of the Long Range Planning Committee of URSI. He serves on advisory boards and committees of a number of organizations. He has received numerous awards, including the Shida Award from the Japanese Ministry of Post and Telecommunications in 1998, the Japan Microwave Prize in 1998, the IEEE Third Millennium Medal in 2000, and the IEEE MTT Distinguished Educator Award in 2000.

Ming C. Wu (S'82–M'83–SM'00) received the M.S. and Ph.D. degrees in electrical engineering from the University of California at Berkeley, in 1985 and 1988, respectively.

From 1988 to 1992, he was Member of the Technical Staff at AT&T Bell Laboratories, Murray Hill, NJ, where he conducted research in high-speed semiconductor lasers and optoelectronics. In 1993, he joined the faculty of Electrical Engineering Department, University of California at Los Angeles, where he is currently a Professor. His current research interests include microelectromechanical aystems (MEMS), MOEMS, microwave photonics, and high-speed optoelectronics. He is the Director of the Multiuniversity Research Initiative (MURI) Center on RF Photonic Materials and Devices sponsored by the Office of Naval Research (ONR), and a member of California NanoSystem Institute (CNSI). He has authored or co-authored more than 100 journal papers, 180 conference papers, contributed one book chapter, and holds eight U.S. patents.

Dr. Wu is a member of the American Physical Society, the Optical Society of America, URSI, and Eta Kappa Nu. He was general co-chair of the IEEE Lasers and Electro-Optics Society (IEEE LEOS) Summer Topical Meeting in 1995 (RF Optoelectronics), 1996, and 1998 (Optical MEMS), and the 1998 International Conference on MOEMS. He has also served on the Program Committees of the OFC, CLEO, MEMS, Optical MEMS, IEDM, and DRC. He received the Packard Foundation Fellowship in 1992 and the Meritorious Conference Paper Award of 1994 GOMAC.

Dalma Novak (S'90–M'91) received the Bachelor of Engineering (electrical) (with first-class honors) and the Ph.D. degree from the University of Queensland, Brisbane, Australia, in 1987 and 1992, respectively.

In 1992, she joined the PRL, Department of Electrical and Electronic Engineering, The University of Melbourne, Melbourne, Australia, where she is currently an Associate Professor and Reader. She is also a Key Researcher in the CRC and Deputy Director of the PRL. She has authored or co-authored over 120 papers in these areas. Her research interests include fiber-wireless communication systems, semiconductor lasers, and high-speed optical networks.

Rodney B. Waterhouse (S'90–M'94) received the B.E. (Hons), M.Eng.Sc. (Research), and Ph.D. degrees from the University of Queensland, Brisbane, Australia, in 1987, 1990, and 1994, respectively.

In 1994, he joined the School of Electrical and Computer Engineering, RMIT University, where he is currently a Senior Lecturer. His research interests include printed antennas, phased arrays, optically distributed wireless systems, and photonic devices for microwave applications. He has authored or co-authored more than 130 papers and holds three patents in these areas. In 2000, RMIT University became a member of the Australian Photonics Cooperative Research Centre (CRC), where he is now a CRC Key Researcher. From mid-2000 to the beginning of 2001, he was a Visiting Professor with the Department of Electrical and Computer Engineering, University of California at Los Angeles, for three months and then a Visiting Researcher in the Photonics Technology Branch, Naval Research Laboratories, Washington, DC, for an additional three months while on his sabbatical.

Dr. Waterhouse is the former chair of the IEEE Victorian Microwave Theory and Techniques Society (MTT-S)/Antennas and Propagation Society (AP-S) Chapter.

Deborah L. Sivco, photograph and biography not available at time of publication.

Alfred Y. Cho (S'57–M'60–SM'79–F'81), photograph and biography not available at time of publication.